

Probing Saturon-like Limits in QCD Systems

Wei Kou^{1, 2, 3, *} and Xurong Chen^{1, 2, 3, †}

¹*Institute of Modern Physics, Chinese Academy of Sciences, Lanzhou 730000, Gansu Province, China*

²*School of Nuclear Science and Technology, University of Chinese Academy of Sciences, Beijing 100049, China*

³*Southern Center for Nuclear Science Theory (SCNT), Institute of Modern Physics, Chinese Academy of Sciences, Huizhou 516000, Guangdong Province, China*

High-occupancy QCD matter enters a saturated regime when its entropy or occupancy approaches the unitarity bound $\sim 1/\alpha$, the “saturon” criterion. We test this criterion for protons and nuclei at small x using analytic and numerical solutions of the BK equation. From these solutions we construct the gluon occupancy $N_g(x)$ and a thermodynamic entropy $S(x)$ via an Unruh-like temperature $T = Q_s/(2\pi)$ and an emergent gluon mass $M_g \sim Q_s$. For protons, both N_g and S rise toward small x yet stay below $1/\alpha_s$ in our baseline setup. For nuclei, by contrast, the nuclear entropy S_A attains the $1/\alpha_s$ benchmark in a small- x window where the proton does not. This singles out nuclei as the natural environment to search for saturon-like behavior and motivates precision small- x measurements and high-occupancy pA and AA collisions.

I. INTRODUCTION

In high-energy quantum field theory, an emerging concept has stimulated renewed consideration of saturation, entropy, and semiclassical behavior: the saturon. First introduced by Dvali et al. [1–4], a saturon refers to a highly occupied composite field configuration that attains maximal entropy under the constraint of unitarity. The thermodynamic properties of saturons, such as entropy-area analogies and thermal-like behavior, evoke parallels with black holes, although they arise within non-gravitational and renormalizable theories. When the occupation number n and the coupling constant α satisfy $n\alpha \sim \mathcal{O}(1)$, the system exhibits semiclassical behavior, and the entropy scales as $S \sim 1/\alpha$, which in four dimensions resembles the Bekenstein-Hawking entropy relation $S \sim R^2$ [5, 6].

Moreover, saturons are not merely theoretical constructs: because their entropy reaches its maximal value, they can be produced in a thermal bath through quantum transitions without exponential suppression. This contrasts with conventional topological solutions or black hole formation mechanisms, which are typically subject to exponential suppression by a Boltzmann factor or dynamical constraints. Such entropy-driven enhancement makes saturons compelling candidates for dark matter and suggests that they may also yield observable signatures in high-energy collisions [7].

The potential connection between the infrared behavior of the strong interaction and gravity has long been a subject of intense discussion. One of the most prominent manifestations of this idea is the application of the Anti-de Sitter/Conformal Field Theory (AdS/CFT) correspondence in strongly interacting theories [8–11]. The rapid development of this framework has led to new interpretations in black hole thermodynamics, quantum field theory, and hadronic physics, particularly by relating certain black hole properties to entanglement and other features emerging in strong interaction studies [12, 13] (See others works related entropy [14–33].). As the fundamental theory of strong interactions, QCD provides a basis for exploring hadron structure and nuclear matter properties. Its infrared dynamics can also be investigated through the mapping of four-dimensional Minkowski field theories onto the boundary of a five-dimensional AdS spacetime. A notable recent example of a concrete connection between gravity and QCD is the so-called BCJ “double copy” relation [34], where gravitational perturbative amplitudes are constructed from QCD amplitudes supplemented by additional kinematic factors. As a distinctive subject of gravitational studies, black holes exhibit certain properties that may find correspondence in investigations of the strong interaction. As discussed in Ref. [12], it is possible to relate the behavior of systems near saturation to both highly occupied graviton states characteristic of black holes and the framework of the Color Glass Condensate (CGC) effective theory [35, 36].

The central focus of this work is to explore saturation phenomena from the perspective of proton structure. It is well established that in high-energy hadrons, such as protons, the number of gluons increases rapidly as the Bjorken- x —the longitudinal momentum fraction carried by gluons—becomes very small. However, when the gluon density reaches a sufficiently high level, nonlinear interactions among gluons, such as gluon-gluon recombination, become significant and inhibit the unbounded growth of gluon density. This phenomenon is referred to as gluon saturation. In other words, the gluon population cannot grow indefinitely without violating unitarity. A central question addressed in this work

* kouwei@impcas.ac.cn

† xchen@impcas.ac.cn (Corresponding Author)

is whether a system constrained by unitarity, such as the saturated gluon system in a proton, can be connected to the concept of a saturon. This concept, introduced by Dvali et al., refers to highly occupied field configurations that reach maximal entropy while respecting unitarity. In Sec. II, we offer a concise review of QCD's nonlinear small- x evolution equations and the phenomenon of gluon saturation within the proton. We also formalize physical quantities such as entropy and occupation number to serve as potential criteria for identifying a system as a saturon. In Sec. III, we present our computed observables and examine the relationship between high-gluon-occupancy protons and saturon behavior. Finally, we provide a summary and outlook. This study introduces a novel perspective on saturation in the proton system, suggesting that, near the saturation threshold, universal behavior can emerge independently of detailed microdynamics or initial conditions. Such a proton state represents a saturated condition comprised of highly occupied soft quanta, sufficient to form a cross section constrained by unitarity [3, 4, 12].

II. FORMALISM

A. Gluon saturation and small- x evolution

A prominent feature of QCD in the high-energy regime is the emergence of high-density partons distributions, a consequence dictated by first principles. Due to the presence of the three-gluon interaction term, radiated gluons can further split into additional gluon fields. The evolution of parton distributions with respect to the photon virtuality Q^2 and the Bjorken scaling variable x is governed by evolution equations, primarily the Dokshitzer-Gribov-Lipatov-Altarelli-Parisi (DGLAP) equation [37–40] and the Balitsky-Fadin-Kuraev-Lipatov (BFKL) equation [41, 42]. The DGLAP equation accurately describes the QCD dynamics of the proton at moderately large x and intermediate to high $Q^2 \gg \Lambda_{\text{QCD}}^2$, while the BFKL equation complements this by capturing the evolution behavior in the small- x regime, where parton densities become significantly enhanced.

The unbounded growth of high-energy gluons is not consistent with physical reality. In practice, as the number of gluons increasingly populates the phase space of the proton, spatial overlap among them becomes inevitable. When the overlapping gluons come sufficiently close, gluon recombination occurs, leading to saturation (See FIG. 1). This nonlinear effect is not accounted for within the framework of the BFKL equation. In fact, the earliest nonlinear corrections to the DGLAP equation were introduced in Refs. [43, 44] and are known as the GLR-MQ equation. Subsequently, the Balitsky-Kovchegov (BK) equation [45–47] was formulated based on the unitarity of the dipole scattering amplitude, incorporating nonlinear terms.

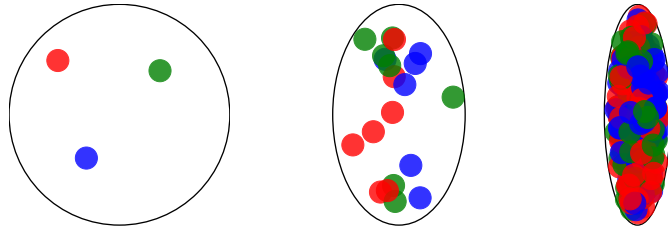


FIG. 1. The gluon density inside the proton increases from low to high energies (from left to right), eventually reaching a state of gluon saturation as a result of overlap and gluon recombination.

B. Balitsky-Kovchegov equation

In this work, we employ the BK equation to characterize the saturation behavior of the proton and compare it with the criteria for a saturon system. The BK equation governs the evolution of the dipole amplitude with rapidity $Y = \ln 1/x$, and in momentum space, it can be expressed as [45, 46]

$$\frac{\partial \mathcal{N}(k, Y)}{\partial Y} = \bar{\alpha}_s \int_0^\infty \frac{d\ell^2}{\ell^2} \left[\frac{\ell^2 \mathcal{N}(\ell, Y) - k^2 \mathcal{N}(k, Y)}{|k^2 - \ell^2|} + \frac{k^2 \mathcal{N}(k, Y)}{\sqrt{4\ell^4 + k^4}} \right] - \bar{\alpha}_s \mathcal{N}^2(k, Y). \quad (1)$$

In this formulation, N_c denotes the number of colors, α_s is the QCD coupling constant, and $\bar{\alpha}_s = \alpha_s N_c / \pi$. In addition, there exists a differential form of the BK equation, expressed using the BFKL kernel $\chi(\lambda)$, as given in Ref. [47]

$$\frac{\partial \mathcal{N}(k, Y)}{\partial Y} = \bar{\alpha}_s \chi \left(-\frac{\partial}{\partial \ln k^2} \right) \mathcal{N}(k, Y) - \bar{\alpha}_s \mathcal{N}^2(k, Y). \quad (2)$$

The BFKL kernel in this context can be represented in terms of the digamma function $\psi(\lambda) = \Gamma'(\lambda)/\Gamma(\lambda)$

$$\chi(\lambda) = \psi(1) - \frac{1}{2} \psi \left(1 - \frac{\lambda}{2} \right) - \frac{1}{2} \psi \left(\frac{\lambda}{2} \right). \quad (3)$$

The two forms of the equation are equivalent, implying that the dipole amplitude is a function of the evolution rapidity $Y(x)$ and the gluon transverse momentum k . Both formulations of the BK equation admit solutions in momentum space and can serve as inputs for calculating scattering amplitudes in diffractive processes as well as proton structure functions. Once the dipole amplitude is obtained from solving the BK equation, one can proceed to compute the unintegrated gluon distribution (UGD) and the gluon number density. Therefore, the solution to the BK equation captures the gluon evolution dynamics in the small- x regime. For the nonlinear integro-differential form of Eq. (1), a Runge-Kutta scheme incorporating integral terms can be employed. In this work, we use the BKsolver algorithm as outlined in Ref. [48], which approximates the integral term using Chebyshev polynomials. This method proves highly effective and allows for both fixed and running coupling scenarios. For the differential form of the BK equation, it is also possible to obtain approximate analytical solutions. By transforming the equation into the form of the Fisher-Kolmogorov-Petrovsky-Piskunov (FKPP) equation [49–55], one can apply techniques developed for nonlinear partial differential equations to perform the analysis.

The solution to the BK equation, along with its characteristic quantity—the saturation scale Q_s^2 —can be directly extracted from the solution itself. From the perspective of analytical analysis, we adopt the homogeneous balance method employed in Refs. [56–59] to solve the BK (or FKPP) equation, which includes treatments for both fixed and running QCD coupling. Details of the solution methodology can be found in the relevant literature. In the fixed coupling (fc) scenario, an analytical solution to the BK equation in momentum space takes the form given as

$$\mathcal{N}_{fc}(L, Y) = \frac{A_0 e^{5A_0 Y/3}}{\left[e^{5A_0 Y/6} + e^{\left[-\theta + \sqrt{A_0/6A_2}(L - A_1 Y) \right]} \right]^2} \quad (4)$$

with $L = \ln(k^2/\Lambda_{\text{QCD}}^2)$, where $A_{0,1,2}$ and θ are fitting parameters. These parameters can be determined using gluon distribution data or proton structure function data [57, 58], in this work we use $A_0 = 33.3$, $A_1 = -58.3$, $A_2 = 26.2$, and $\theta = -3.09$ [57]; however, as this is not the primary focus of the present study, we do not elaborate further. To extract the saturation scale Q_s , which corresponds to the transverse momentum at the saturation threshold, we directly utilize the analytical solution via the method described in Ref. [57]

$$Q_s^2(Y) = \Lambda_{\text{QCD}}^2 e^{(A_1 + 5\sqrt{A_0 A_2/6})Y}. \quad (5)$$

The associated parameters are consistent with those of the solution, and Λ_{QCD} , representing the infrared cutoff, is taken to be 0.2 GeV.

For the case of running coupling (rc), the details of the treatment using the homogeneous balance method can similarly be found in Ref. [59]. In this work, we adopt the saturation scale prescription (SSP), whereby the running coupling scale is identified with the saturation scale Q_s . This choice reflects the characteristic momentum of gluons in the saturated regime and offers improved performance in describing the small- x proton structure function F_2 . The scale-dependent running coupling constant is expressed as [59]

$$\bar{\alpha}_s(Q_s^2) = \frac{1}{b \ln \frac{Q_s^2}{\Lambda_{\text{QCD}}^2}}, \quad (6)$$

where $b = (11N_c - 2N_f)/12N_c$ with the number of color N_c and number of flavor N_f , respectively.

The saturation scale Q_s is proportional to the gluon density and thus exhibits a positive correlation with the rapidity Y . This relationship can be established through [60]

$$Q_s^2(Y) = \Lambda_{\text{QCD}}^2 e^{\sqrt{cY}} \quad (7)$$

with the free parameter c . This is consistent with the reasoning behind Eq. (5), where, upon assuming a specific scale for the coupling constant, the analytical solution to the BK equation in the running coupling scenario can also be obtained using the homogeneous balance method. The explicit form is given as [59]

$$N_{rc}(L, Y) = \frac{A_0 \exp \left[2\theta + 2 \frac{\left(\frac{\sqrt{6}A_0 A_1}{\sqrt{A_2}} + 5A_0 \right) \sqrt{cY}}{3bc} \right]}{\left\{ \exp \left[\theta + \frac{\left(\frac{\sqrt{6}A_0 A_1}{\sqrt{A_2}} + 5A_0 \right) \sqrt{cY}}{\sqrt{A_2}} \right] + \exp \left[\frac{\sqrt{A_0} L}{\sqrt{6}A_2} \right] \right\}^2}, \quad (8)$$

Similarly, this analytical solution contains free parameters that must be determined by fitting to experimental data. Specifically, in the case of running coupling, the parameters of the analytical solution are obtained by fitting to the experimental data of the structure function [61, 62], yielding $A_0 = 6.98$, $A_1 = -8.46$, $A_2 = 2.95$, $c = 3.11$, and $\theta = -2.76$.

A detailed discussion of the numerical solutions to the BK equation is beyond the scope of this work; here we briefly outline the method for extracting the saturation scale Q_s^2 from such solutions. Following the approach proposed in Refs. [48, 63], it is reasonable to define the transverse momentum corresponding to the saturated dipole amplitude at different $Y(x)$ as the saturation scale, i.e., by imposing the condition $\mathcal{N}(Y, Q_s^2(Y)) = \mathcal{N}_0 \sim \kappa$. Clearly, the value of Q_s depends on the chosen threshold κ . Investigating how different values of κ affect the extracted saturation scale is of interest, and the resulting behavior should be compared to the asymptotic analytical behavior reported in Refs. [49, 50]. Notably, for $\kappa = 1$, the numerical solutions obtained using BKsolver [48] reproduce the expected asymptotic behavior well in both fixed and running coupling scenarios.

Figure 2 presents both the analytical and numerical solutions of the BK equation with fixed and running coupling, obtained using the methods described above. The figure displays the distribution of the dipole amplitude as a function of gluon transverse momentum for various values of x (In each subfigure, the four curves from left to right correspond to $x = 10^{-1}, 10^{-3}, 10^{-5}, 10^{-7}$, respectively.). It is evident that all solutions exhibit wavefront-like profiles, a feature connected to the statistical properties underlying the BK equation. The analytical solutions, in particular, provide explicit functional forms for these traveling wave solutions. Furthermore, FIG. 3 illustrates the evolution of the saturation scale Q_s^2 as a function of x for different solution schemes. The solid line, dashed line, dash-dotted line, and dotted line correspond to the four respective solutions. While some discrepancies exist between the extracted saturation scales across methods, due to differing assumptions in solving the equation or defining the saturation condition, the general trend remains consistent: Q_s^2 increases as x decreases.

C. Saturons, occupation number and entropy

As discussed earlier, we aim to determine whether high-occupancy systems exhibit distinctive dynamical properties at the critical point. Taking black holes as an example, critical packing leads to the emergence of a large number of gapless modes, which correspond to specific microstate entropy S . Among the relations involving entropy, the most significant is its dependence on the system coupling constant $\alpha(Q_s)$ with saturation scale Q_s at the critical point. This correspondence was proposed in Refs. [1–3] and implies an upper bound on the microstate entropy and occupation number of a system

$$S_{\max} \simeq N_{\max} = \frac{1}{\alpha(Q_s)}. \quad (9)$$

At the same time, Ref. [3] further proposed that the correlation between unitarity-preserving saturation and the entropy bound (9) is inherently nonperturbative and cannot be circumvented through resummation schemes within perturbative frameworks. Moreover, any system that reaches this entropy limit exhibits, to some extent, universal features shared with black holes. In the relevant literature, the connection between black holes and analogous saturated objects in other physical systems has been established, including states in gauge theories with a large number of colors.

Several studies have suggested a correspondence between black holes and the CGC formed in high-energy matter collisions, the latter being a high-occupancy condensate permitted within the framework of QCD. Although the critical behavior of QCD differs from that of gravity, they share common features in terms of critical packing. Both the black hole state and the CGC state emerge as outcomes of the classicalization and unitarization of the $2 \rightarrow N$ amplitude in the high-energy Regge limit of gravity or QCD [12]. The interpretation of black holes and other field-theoretic systems as saturated states has been extensively discussed in the literature. Our focus here is on the nucleon system, more precisely the high-energy proton parton distribution system governed by QCD. We investigate whether it can be regarded as a saturated state, and examine its implications for microscopic entropy as well as the definition of high-occupancy states.

One may consider a highly occupied proton, namely the gluon distribution inside the proton in the small- x region. This distribution can be described within the framework of the BK equation through the relation between the dipole scattering amplitude and the UGD. The gluon occupancy N_g at high energies can be expressed in terms of the gluon multiplicity distribution produced in collision processes, given as [36, 64]

$$N_g(x, \mathbf{k}_\perp, \mathbf{x}_\perp) \equiv \frac{(2\pi)^3}{2(N_c^2 - 1)} x \frac{dN_{\text{gluon}}}{dx d^2\mathbf{k}_\perp d^2\mathbf{x}_\perp}, \quad (10)$$

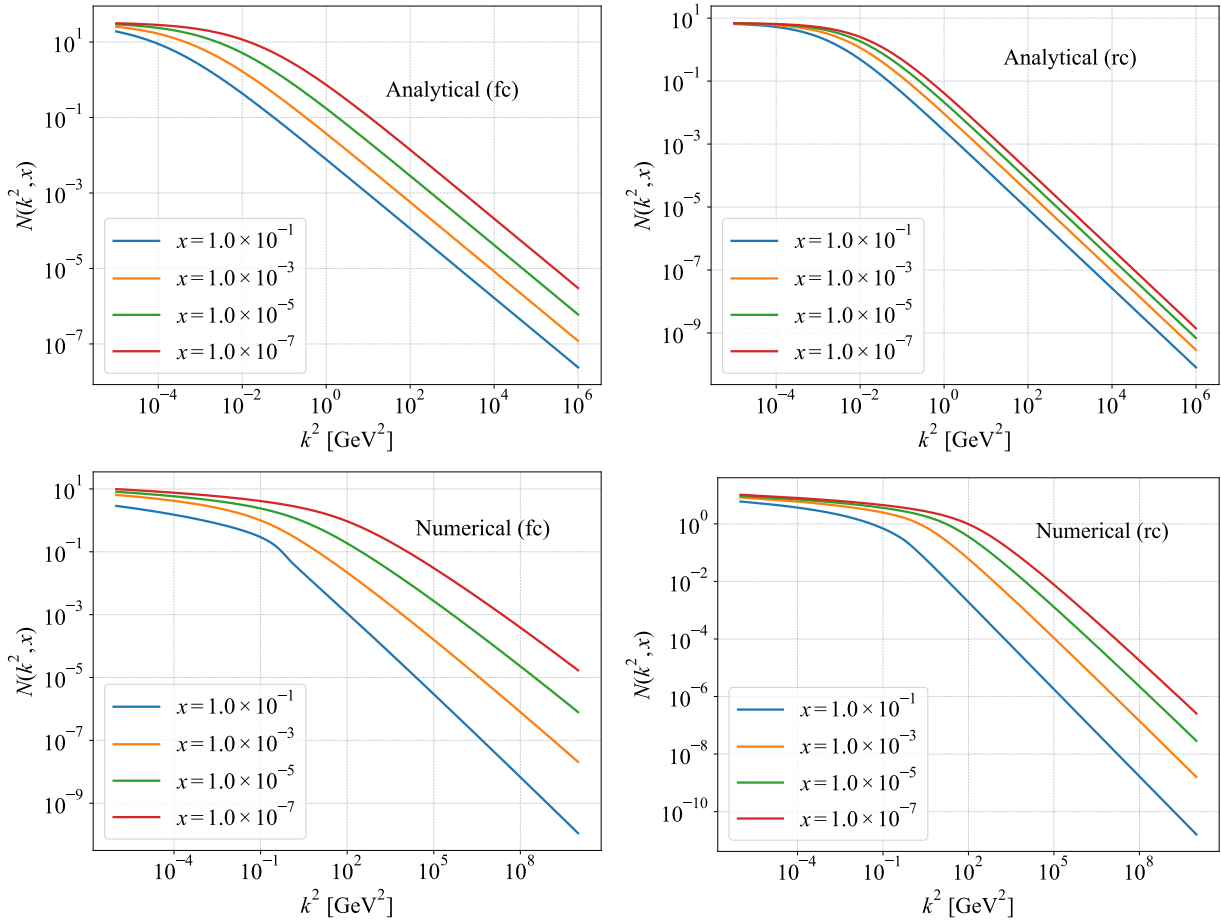


FIG. 2. From left to right and top to bottom, the panels correspond to the analytical and numerical solutions of the BK equation in the fixed and running coupling cases, respectively. The solution methods follow [48, 57, 59]. In each subfigure, the four curves from left to right represent $x = 10^{-1}, 10^{-3}, 10^{-5}, 10^{-7}$, respectively.

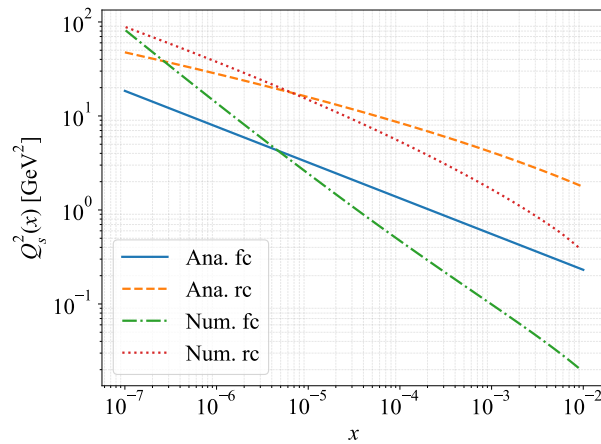


FIG. 3. The variation of the extracted saturation scale Q_s^2 with respect to x under different schemes is shown. The solid line, dashed line, dash-dotted line, and dotted line correspond to the four respective solutions.

where \mathbf{k}_\perp and \mathbf{x}_\perp are transverse momentum and impact parameter of gluon, respectively. It means the the UGD per unit transverse area. A frequently used simplified estimate takes the form:

$$N_g(x, Q^2) \simeq \frac{1}{Q^2} \frac{xG(x, Q^2)}{\pi R^2}, \quad (11)$$

where xG is the gluon distribution and can be written by the integration of UGD \mathcal{F} , $xG(x, Q^2) = \int^{Q^2} \frac{dk^2}{k^2} \mathcal{F}(x, k^2)$. The integral over the transverse impact parameter is generally interpreted as the transverse cross section of the boosted proton, πR^2 , with proton radius $R = 0.84$ fm. Regarding the explicit form of the UGD, one approach derived from [65] expresses it in terms of the dipole amplitude \mathcal{N} obtained from the solution of the BK equation

$$\mathcal{F}(x, k^2) = \frac{N_c R^2}{\alpha_s \pi} \left(1 - k^2 \frac{d}{dk^2}\right)^2 k^2 \mathcal{N}(k^2, x). \quad (12)$$

We now turn to the discussion of how to define the concept of saturation entropy for the proton in a high gluon occupancy regime. A potential approach to resolving the entropy of such a highly occupied system was proposed in [66, 67] and subsequently applied in [14] to address entropy production in high-energy collisions. This perspective originates from the partonic picture of QCD, where the thermalization of a hadron is associated with a temperature linked to its saturation scale

$$T = \frac{Q_s(x)}{2\pi}, \quad (13)$$

where x stands for a longitudinal momentum fraction of hadron carried by a parton. This connection is established through the well-known Unruh effect [68]. A concise formulation of the Unruh effect states that an observer undergoing constant acceleration a perceives a thermal bath with temperature $T = a/2\pi$ in their own rest frame. When applied to off-shell gluons being radiated, this suggests a deceleration effect in the transverse-momentum-dependent UGD. By analyzing gluon deceleration in a uniform chromoelectric field, one finds that the characteristic acceleration is compatible in magnitude with the saturation scale [66, 69], such that $a = Q_s(x)$

In addition to temperature, a complete thermodynamic definition of entropy requires a description of energy. Inspired by [46, 47], we associate the emergent mass generated through the nonlinear evolution of gluons with the saturation scale. Specifically, this mass is taken to be proportional to the saturation scale, thereby avoiding divergences in the gluon propagator. Furthermore, it has been suggested that gauge-invariant gluons may acquire a dynamical mass due to nonlinear effects (see Refs. [70, 71] and references therein). Accordingly, one may express the mass of a single gluon as [14]

$$M_g(x) = Q_s(x). \quad (14)$$

Based on the definitions of gluon mass and system temperature discussed above, one can formulate a coarse-grained entropy, as implied by the fundamental laws of thermodynamics, under the assumption that the system volume remains approximately constant. Using the energy- or the effective mass of the gluons-together with the temperature derived from the Unruh effect, the entropy is found to satisfy the following differential equation

$$dM = dE = TdS, \quad (15)$$

here, the mass M can be interpreted as the total emergent mass of all gluons, namely, the total energy of N_g gluons with individual mass $M_g(x)$, such that $M(x) = N_g(x)M_g(x)$. Naturally, the longitudinal momentum fraction x carried by the gluons should be accounted for in the dependence of the above quantities, and it can serve as one of the scaling variables for the entropy. By introducing the Unruh acceleration $a = Q_s(x)$, the differential expression for the entropy can then be obtained directly from Eq. (13) as follows:

$$dS = 2\pi \frac{d[N_g(x)M_g(x)]}{Q_s(x)}. \quad (16)$$

For simplicity, the lowest entropy state S_0 can be set to zero. All integration constants can be absorbed into quantities related to the gluon occupation number, which may be determined from experimental data or global QCD fits. It is important to emphasize that, in this analysis, the gluon occupation number (or gluon density) is obtained from the solution of the BK equation. Ultimately, the thermodynamic entropy of the system constructed via the Unruh effect and the emergent gluon mass takes the following form:

$$S(x) \simeq \pi N_g(x) \ln \frac{Q_s^2(x)}{\Lambda_{\text{QCD}}^2}. \quad (17)$$

The thermodynamic entropy of the high-occupancy gluon state obtained above is consistent with the conclusion presented in [15], where a simplified analytic expression for the gluon distribution based on the Golec-Biernat Wuesthoff (GBW) model [72] yields a result that matches the entanglement entropy derived from DIS [13, 18, 73–78].

The properties of black holes as saturons systems have been extensively studied. We now turn to the question of whether a highly saturated proton, characterized by a large gluon occupation number in its interior, can exhibit features analogous to those of black holes. As previously discussed, saturons systems display certain universal behaviors near the critical regime. The Bekenstein-Hawking entropy of a black hole suggests that for a black hole of radius R , the entropy scales as $S \sim A_{\text{era}}/G_{\text{gr}}$,

where G_{gr} denotes Newton's gravitational constant and has dimensions of R^{d-2} . The saturation property of black holes leads to the entropy saturating the Bekenstein-Hawking bound, yielding $S \sim 1/\alpha_{gr}$ with $\alpha_{gr} = G_{gr}/R^{d-2}$.

We now consider the internal dynamics of a highly saturated proton governed by QCD. The gluon distribution at the saturation scale $Q = Q_s(x)$, denoted by $xG(x, Q_s(x))$, can be obtained by integrating the UGD over transverse momentum. The UGD itself is derived from the solution of the BK equation via the dipole scattering amplitude and Eq. (12). It can be shown that the gluon distribution obtained from the UGD satisfies $xG \sim A_\perp/\alpha_s$ [15, 72], where $A_\perp = \pi R^2$ represents the transverse area of the boosted proton. The gluon occupation number N_g is related to xG through Eq. (11) and ultimately enters the expression for the system's thermodynamic entropy via Eq. (17), resulting in the scaling

$$S(x) \sim N_g(x) \sim 1/\alpha_s. \quad (18)$$

This provides the basis for considering the high-energy, high-occupancy gluon state in the proton as a saturons system. In contrast to the gravitational case, the relevant coupling constant is now the QCD strong coupling α_s , which depends on the saturation scale as $\alpha_s \sim \alpha_s(Q_s^2)$.

D. From proton to nucleus: Glauber-Gribov-Mueller Scheme

It is also worth mentioning the extension of the nucleon UGD to the nuclear case, since the nuclear mass number (A) can enhance the gluon distribution in the high-saturation regime of a nucleus, in line with the CGC picture. In this work we adopt a simple scheme that maps the UGD from a single proton to a high-mass-number nucleus (e.g., Pb), with the goal of straightforwardly comparing its saturation criterion with that of a single nucleon. Multiple scattering in a dense nuclear target can be described by the Glauber-Gribov-Mueller (GGM) approximation [79–84]. The nuclear saturation scale grows with mass number [36, 84]

$$Q_{s,A}^2(x) \simeq A^{1/3} Q_{s,p}^2(x), \quad R_A = r_0 A^{1/3}, \quad (19)$$

where $Q_{s,p} = Q_s$ in Eq. (5) represents the nucleon saturation scale, R_A is the nuclei radius with mass number A and $r_0 = 1.2$ fm.

Unlike the dipole scattering amplitude for the proton – i.e., the solution of the BK equation – the nuclear dipole amplitude is taken in the eikonalized GGM form [80, 81, 85]

$$N_A(r, b, x) = 1 - \exp \left[-\frac{1}{2} \sigma_{\text{dip}}^p(r, x) T_A(b) \right]. \quad (20)$$

Here, T_A denotes the Woods-Saxon nuclear thickness profile [86], which together with the dipole-proton scattering cross section σ_{dip}^p composes the dipole-nucleus scattering amplitude.

The σ_{dip}^p is obtained from a Hankel transform of the proton UGD, which maps momentum-space information into coordinate space. The proton UGD has the form given above, explicitly written as [84, 87]

$$\sigma_{\text{dip}}^p(x, r) = \frac{8\pi\alpha_s}{N_c R_p^2} \int_0^\infty dk \frac{1 - J_0(kr)}{k^3} \mathcal{F}_p(x, k^2) \quad (21)$$

Note that N_A is the nuclear amplitude in the fundamental representation. To move to the adjoint representation while enforcing unitarity [14], deform it as $N_G(r, b, x) = 2N_A(r, b, x) - N_A^2(r, b, x)$. Then integrate over the impact parameter b ; applying the gradient and performing a Fourier transform yields the UGD for the nuclear case

$$\mathcal{F}_A(x, k^2) = \frac{N_c R_A^2 \pi}{2\alpha_s^2 C_F} k^2 \phi_A(k, x) \quad (22)$$

with

$$\phi_A(k, x) = \frac{C_F \alpha_s}{(2\pi)^3} \int d^2 r e^{-ik \cdot r} \nabla_r^2 \left[\int d^2 b N_G(r, b, x) \right]. \quad (23)$$

With the nuclear UGD in hand, one can, by analogy with the proton case, compute the nuclear gluon occupancy, thermodynamic entropy, and related quantities. This enables a comparison with the saturation criterion. We will present a more detailed discussion in the next section.

III. RESULTS AND DISCUSSIONS

Up to this point, we have formally discussed the potential of high-energy protons to serve as candidates for saturons. However, accurately determining the properties of saturons from gluon distributions remains a substantial challenge, owing to higher-order corrections in the small- x gluon evolution within the proton and certain non-perturbative effects. Additionally, the number of gluons radiated by a single proton is considerably smaller than that found in the highly saturated color-charge states produced in heavy-ion collisions. Nevertheless, it is of significant interest to assess whether protons can be identified as saturons through their gluon distributions. A suitable framework for describing saturated protons is provided by the small- x

QCD evolution equations, specifically the nonlinear BK/JIMWLK equations. These equations can be expressed in terms of the gluon occupation number, with the explicit nonlinear form given by $\partial_Y N_g = \omega \alpha_s N_g - \alpha_s N_g^2$, where ω is a number of order unity [36]. The nonlinear term originates from the gluon recombination process $gg \rightarrow g$. Upon reaching saturation, the gluon occupation number should become independent of the rapidity evolution variable Y , leading to $N_g \sim 1/\alpha_s$. This provides a criterion for identifying saturon systems directly from the evolution equation itself, namely Eq. (18).

A. Proton case

Through the mean-field approximation of the nonlinear evolution equation, namely the momentum-space BK equation, both its analytical and numerical solutions for the dipole amplitude can be related to the gluon distribution via the definition of the UGD. This connection allows the determination of the gluon occupation number and the corresponding thermodynamic entropy, as given in Eqs (11-17).

Following the above framework, the numerical results are presented in Fig. 4. This includes both analytical and numerical solutions obtained with fixed and running coupling, showing the distributions of the gluon occupation number (blue solid lines) and the corresponding thermodynamic entropy (red dashed lines) as functions of x . For comparison with the coupling strength, we also include the coupling constant curve as a black dotted-dashed line. The fixed coupling is set to $\alpha_s = 0.2$, while the running coupling is determined using the one-loop β -function.

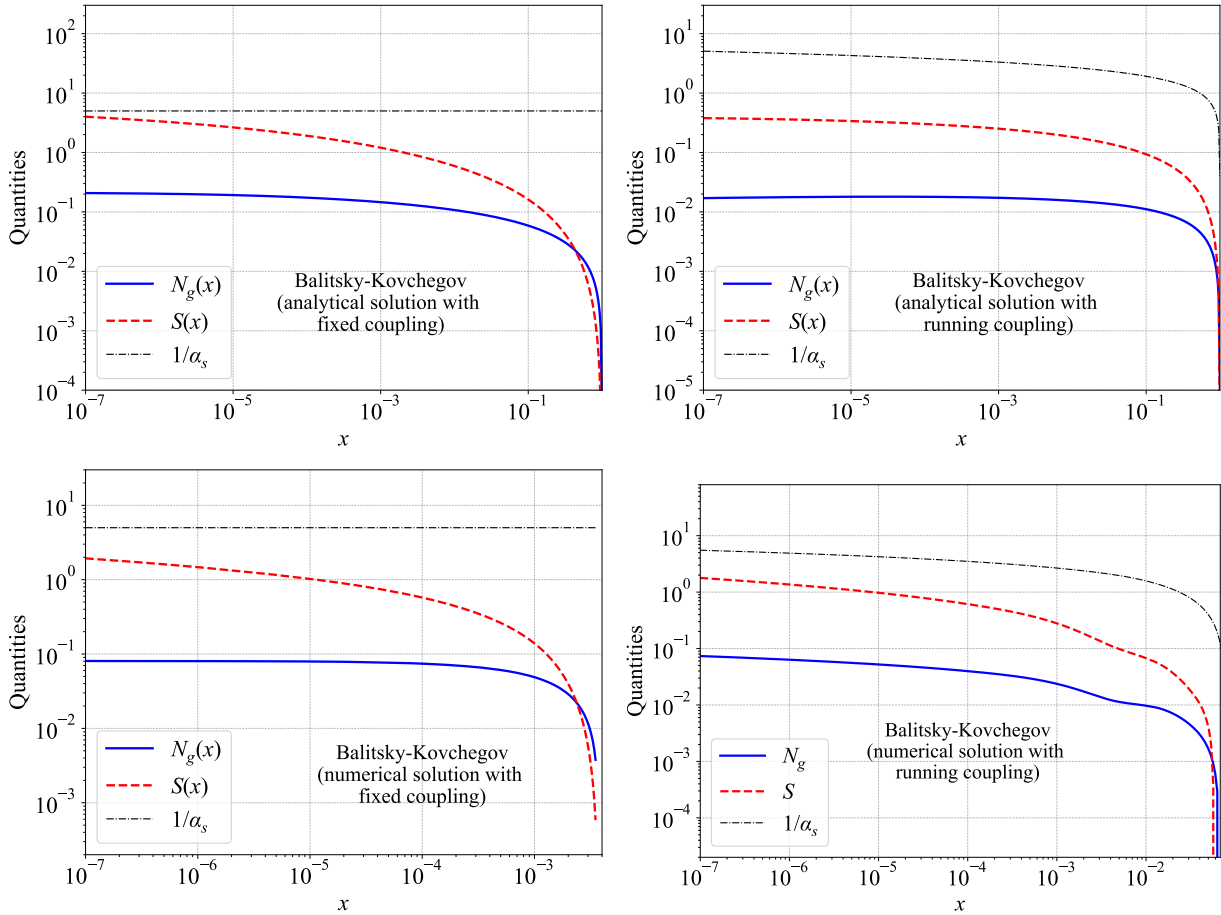


FIG. 4. The four subplots, arranged from left to right and top to bottom, represent respectively: the analytical solution of the BK equation with fixed coupling, the analytical solution with running coupling, the numerical solution with fixed coupling, and the numerical solution with running coupling. Each panel displays the resulting gluon occupation number and the associated entropy.

The parameter choices for all results shown in the figure are specified in the main text and are taken from the corresponding references. The four subplots, arranged from left to right and top to bottom, represent respectively: the analytical solution of the BK equation with fixed coupling, the analytical solution with running coupling, the numerical solution with fixed coupling, and the numerical solution with running coupling. Each panel displays the resulting gluon occupation number and

the associated entropy. It is observed that in all cases, even down to $x = 10^{-7}$ —well below the kinematic reach of current DIS experiments—neither the entropy nor the gluon occupation number approaches the inverse coupling constant, $1/\alpha_s$. One important reason for this is the presence of approximations in the construction of the entropy, and the omission of higher-order corrections in the evolution equations.

B. Nuclear case

A simple estimate is needed to assess how much a nucleus can enhance quantities such as entropy. We give a single example: the proton dipole amplitude is taken from an analytic solution of the BK equation and extended to the nuclear case using the GGM scheme. We choose a mass number $A = 208$, corresponding to a lead nucleus. Using the same numerical procedure and parameter settings as for the proton (changing only the target from proton to nucleus ($A = 208$) and fixing the coupling at $\alpha_s = 0.2$), we obtain the nuclear target's gluon occupancy $N_g(x)$ and thermodynamic entropy $S(x)$. Figure 5 displays these two curves, with the reference line $1/\alpha_s$ overlaid (the same criterion as in the proton case). As seen in the figure, compared with

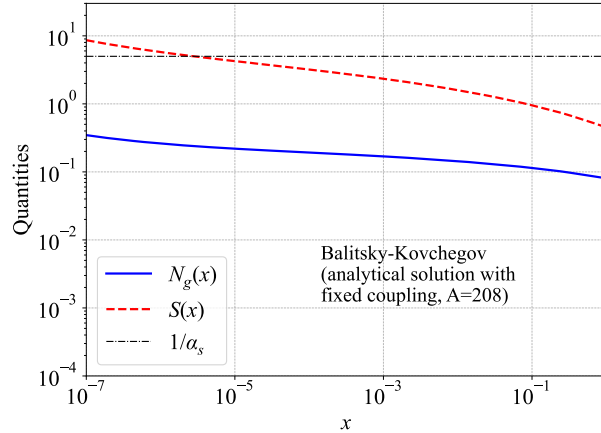


FIG. 5. Gluon occupancy $N_g(x)$ and thermodynamic entropy $S(x)$ for the nucleus ($A = 208$) at fixed coupling; the black horizontal line denotes the criterion $(1/\alpha_s)$.

the proton result, under the x -dependent growth of the entropy, the thermodynamic entropy of a highly occupied lead nucleus reaches the saturation criterion $(1/\alpha_s)$ at around $x \sim 10^{-6}$. This indicates that the nucleus indeed enhances the entropy, mainly through the increase of the transverse radius after the high-energy boost (set by the nuclear radius) and the amplification of the nuclear saturation scale. However, this comparison has limitations, such as the choice of the dipole-amplitude form and uncertainties from nuclear geometric parameters. In this section we use fixed coupling and neglect detailed impact-parameter dependence and higher-order corrections, so the “nucleus reaches while the proton does not” criterion should be regarded as a conservative, trend-level conclusion.

C. Discussions

Based on the results presented above and under the assumptions considered, while both the formal structure and the intrinsic nature of nonlinear QCD evolution at small x appear to support the prospect of the proton as a candidate saturon system, current evaluations—whether from the perspective of gluon occupation number or thermodynamic entropy—indicate that the criteria required to reach the upper bound for saturon identification remain stringent. This necessitates collisions at higher energies and gluonic states with greater occupation densities. In contrast, once the same analysis chain is applied to nuclear targets (fixed coupling, identical numerical settings otherwise), the nuclear curves rise faster. The resulting nuclear entropy $S_A(x)$ approaches and, within the uncertainties of our inputs, can reach the benchmark line $1/\alpha_s$ in a small- x window where the proton stays below. This qualitative separation is stable against reasonable variations of the Q_s extraction threshold, geometric inputs, and numerical smoothing; these choices primarily shift the apparent crossing point but do not invert the ordering. Encouragingly, some studies have already explored the correspondence between black hole saturons and the CGC framework [12]. Portions of those discussions align conceptually with the present work, and notably, they propose a role for Goldstone modes arising from the breaking of Poincaré symmetry. The breaking of Poincaré invariance in this context fundamentally originates from the presence of a hard scale, which characterizes the transition from a dilute partonic gas with a spectral gap to an over-occupied, highly saturated classical field. Partons with momenta below this scale become screened, and high-twist effects become significant. This screening of partonic modes disrupts the translational invariance of the partonic gas, analogous

to the breaking of Poincaré symmetry in black holes, which gives rise to a Goldstone scale characterized by $f = m_{\text{Planck}}$ with Planck mass m_{Planck} [3]. However, in the case of QCD, the precise form and interpretation of such a Goldstone scale remain open to further investigation.

IV. CONCLUSION AND OUTLOOK

In this work, we explored whether a high-energy proton in the small- x regime could qualify as a *saturon*-a highly occupied field configuration that maximizes entropy under unitarity constraints, in analogy with black holes. We derived the gluon occupation number $N_g(x)$ and a thermodynamic entropy $S(x)$ based on analytical and numerical solutions to the BK equation (with both fixed and running coupling), supplemented with an Unruh-inspired temperature $T = Q_s/(2\pi)$ and an emergent gluon mass $M_g \sim Q_s$. Our findings indicate that although both N_g and S increase as x decreases, even down to $x \sim 10^{-7}$, they remain significantly below the theoretical saturon bound $1/\alpha_s$. This suggests that while the proton exhibits nonlinear saturation dynamics, under the current theoretical framework it does not reach the critical maximal occupancy characteristic of a saturon. After extending the same framework to nuclear targets at fixed coupling, the nuclear entropy $S_A(x)$ rises more sharply and, in our numerical study, can reach the $1/\alpha_s$ benchmark in a region where the proton does not. This proton–nucleus contrast identifies nuclei as more favorable environments to probe saturon-like behavior in QCD. Moreover, exploring the connection between the proton and black holes from the perspective of entanglement entropy offers a promising avenue [13]. Notably, some studies have already applied the entanglement-based definition originally proposed for black holes to DIS processes involving protons.

To advance toward the saturon regime, we propose two complementary pathways. On the theoretical front, it is essential to incorporate higher-order QCD corrections-such as NLO effects or small- x resummations-and to explore alternative entropy constructs, particularly entanglement entropy, which may more accurately capture the gluonic microstate structure. Investigating symmetry-breaking phenomena in the saturated regime, such as emergent Goldstone-like modes, may also uncover universal behavior reminiscent of saturon systems.

From experimental and phenomenological perspective, heavy-ion collisions offer a promising environment to probe truly over-occupied gluonic systems. The CGC effective theory, which describes saturated gluon matter at high energy, has been successfully applied to model the initial stages of heavy-ion collisions at RHIC and the LHC [88]. These systems, in which gluon densities are far higher than in isolated protons, may approach saturon-like occupancy. Additionally, future facilities such as the Electron-Ion Collider (EIC) are expected to explore deep small- x regimes in both proton and nuclear targets, with unprecedented luminosity and kinematic reach [89–92]. A comprehensive study-spanning proton-proton, proton-nucleus, and nucleus-nucleus collisions-of gluon saturation, entropy production, and correlation patterns could shed light on whether any QCD system realizes saturon-like behavior. Such investigations might reveal deep connections between hadronic saturation dynamics and gravitational entropy bounds.

ACKNOWLEDGMENTS

This work has been supported by the National Key R&D Program of China (Grant NO. 2024YFE0109800 and 2024YFE0109802).

[1] G. Dvali, Area Law Saturation of Entropy Bound from Perturbative Unitarity in Renormalizable Theories, *Fortsch. Phys.* **69**, 2000090 (2021), arXiv:1906.03530 [hep-th].

[2] G. Dvali, Unitarity Entropy Bound: Solitons and Instantons, *Fortsch. Phys.* **69**, 2000091 (2021), arXiv:1907.07332 [hep-th].

[3] G. Dvali, Entropy Bound and Unitarity of Scattering Amplitudes, *JHEP* **03**, 126, arXiv:2003.05546 [hep-th].

[4] G. Dvali, Bounds on quantum information storage and retrieval, *Phil. Trans. A. Math. Phys. Eng. Sci.* **380**, 20210071 (2021), arXiv:2107.10616 [hep-th].

[5] J. D. Bekenstein, Black holes and entropy, *Phys. Rev. D* **7**, 2333 (1973).

[6] S. W. Hawking, Particle Creation by Black Holes, *Commun. Math. Phys.* **43**, 199 (1975), [Erratum: *Commun. Math. Phys.* 46, 206 (1976)].

[7] G. Dvali, Saturon Dark Matter, (2023), arXiv:2302.08353 [hep-ph].

[8] G. 't Hooft, A Planar Diagram Theory for Strong Interactions, *Nucl. Phys. B* **72**, 461 (1974).

[9] A. M. Polyakov, Quantum Geometry of Bosonic Strings, *Phys. Lett. B* **103**, 207 (1981).

[10] J. M. Maldacena, The Large N limit of superconformal field theories and supergravity, *Adv. Theor. Math. Phys.* **2**, 231 (1998), arXiv:hep-th/9711200.

[11] O. Aharony, S. S. Gubser, J. M. Maldacena, H. Ooguri, and Y. Oz, Large N field theories, string theory and gravity, *Phys. Rept.* **323**, 183 (2000), arXiv:hep-th/9905111.

[12] G. Dvali and R. Venugopalan, Classicalization and unitarization of wee partons in QCD and gravity: The CGC-black hole correspondence, *Phys. Rev. D* **105**, 056026 (2022), arXiv:2106.11989 [hep-th].

- [13] W. Kou, X. Wang, and X. Chen, Page entropy of a proton system in deep inelastic scattering at small x, *Phys. Rev. D* **106**, 096027 (2022), arXiv:2208.07521 [hep-ph].
- [14] K. Kutak, Gluon saturation and entropy production in proton–proton collisions, *Phys. Lett. B* **705**, 217 (2011), arXiv:1103.3654 [hep-ph].
- [15] K. Kutak, Entanglement entropy of proton and its relation to thermodynamics entropy, (2023), arXiv:2310.18510 [hep-ph].
- [16] P. Caputa and K. Kutak, Krylov complexity and gluon cascades in the high energy limit, *Phys. Rev. D* **110**, 085011 (2024), arXiv:2404.07657 [hep-ph].
- [17] G. Chachamis, M. Hentschinski, and A. Sabio Vera, Von Neumann entropy and Lindblad decoherence in the high-energy limit of strong interactions, *Phys. Rev. D* **109**, 054015 (2024), arXiv:2312.16743 [hep-th].
- [18] M. Hentschinski, D. E. Kharzeev, K. Kutak, and Z. Tu, QCD evolution of entanglement entropy, *Rept. Prog. Phys.* **87**, 120501 (2024), arXiv:2408.01259 [hep-ph].
- [19] Y. Hatta and J. Montgomery, Maximally entangled gluons for any x, *Phys. Rev. D* **111**, 014024 (2025), arXiv:2410.16082 [hep-ph].
- [20] A. Dumitru, A. Kovner, and V. V. Skokov, Entanglement entropy of the proton in coordinate space, *Phys. Rev. D* **108**, 014014 (2023), arXiv:2304.08564 [hep-ph].
- [21] G. S. Ramos and M. V. T. Machado, Investigating the QCD dynamical entropy in high-energy hadronic collisions, *Phys. Rev. D* **105**, 094009 (2022), arXiv:2203.10986 [hep-ph].
- [22] L. S. Moriggi, G. S. Ramos, and M. V. T. Machado, Multiplicity dependence of the pT-spectra for identified particles and its relationship with partonic entropy, *Phys. Rev. D* **110**, 034005 (2024), arXiv:2405.01712 [hep-ph].
- [23] G. S. Ramos and M. V. T. Machado, Investigating entanglement entropy at small- x in DIS off protons and nuclei, *Phys. Rev. D* **101**, 074040 (2020), arXiv:2003.05008 [hep-ph].
- [24] R. Peschanski, Dynamical entropy of dense QCD states, *Phys. Rev. D* **87**, 034042 (2013), arXiv:1211.6911 [hep-ph].
- [25] N. Armesto, F. Dominguez, A. Kovner, M. Lublinsky, and V. Skokov, The Color Glass Condensate density matrix: Lindblad evolution, entanglement entropy and Wigner functional, *JHEP* **05**, 025, arXiv:1901.08080 [hep-ph].
- [26] D. Neill and W. J. Waalewijn, Entropy of a Jet, *Phys. Rev. Lett.* **123**, 142001 (2019), arXiv:1811.01021 [hep-ph].
- [27] A. Kovner, M. Lublinsky, and M. Serino, Entanglement entropy, entropy production and time evolution in high energy QCD, *Phys. Lett. B* **792**, 4 (2019), arXiv:1806.01089 [hep-ph].
- [28] Y. Liu, M. A. Nowak, and I. Zahed, Mueller’s dipole wave function in QCD: Emergent Koba-Nielsen-Olesen scaling in the double logarithm limit, *Phys. Rev. D* **108**, 034017 (2023), arXiv:2211.05169 [hep-ph].
- [29] Y. Liu, M. A. Nowak, and I. Zahed, Rapidity evolution of the entanglement entropy in quarkonium: Parton and string duality, *Phys. Rev. D* **105**, 114028 (2022), arXiv:2203.00739 [hep-ph].
- [30] Y. Liu, M. A. Nowak, and I. Zahed, Spatial entanglement in two-dimensional QCD: Renyi and Ryu-Takayanagi entropies, *Phys. Rev. D* **107**, 054010 (2023), arXiv:2205.06724 [hep-ph].
- [31] Y. Liu, M. A. Nowak, and I. Zahed, Universality of Koba-Nielsen-Olesen scaling in QCD at high energy and entanglement, (2023), arXiv:2302.01380 [hep-ph].
- [32] A. Stoffers and I. Zahed, Holographic Pomeron and Entropy, *Phys. Rev. D* **88**, 025038 (2013), arXiv:1211.3077 [nucl-th].
- [33] P. Asadi and V. Vaidya, 1+1D hadrons minimize their biparton Renyi free energy, *Phys. Rev. D* **108**, 014036 (2023), arXiv:2301.03611 [hep-th].
- [34] Z. Bern, J. J. M. Carrasco, and H. Johansson, New Relations for Gauge-Theory Amplitudes, *Phys. Rev. D* **78**, 085011 (2008), arXiv:0805.3993 [hep-ph].
- [35] E. Iancu, A. Leonidov, and L. McLerran, The Color glass condensate: An Introduction, in *Cargese Summer School on QCD Perspectives on Hot and Dense Matter* (2002) pp. 73–145, arXiv:hep-ph/0202270.
- [36] F. Gelis, E. Iancu, J. Jalilian-Marian, and R. Venugopalan, The Color Glass Condensate, *Ann. Rev. Nucl. Part. Sci.* **60**, 463 (2010), arXiv:1002.0333 [hep-ph].
- [37] Y. L. Dokshitzer, Calculation of the Structure Functions for Deep Inelastic Scattering and e+ e- Annihilation by Perturbation Theory in Quantum Chromodynamics., *Sov. Phys. JETP* **46**, 641 (1977).
- [38] V. N. Gribov and L. N. Lipatov, Deep inelastic e p scattering in perturbation theory, *Sov. J. Nucl. Phys.* **15**, 438 (1972).
- [39] V. N. Gribov and L. N. Lipatov, e+ e- pair annihilation and deep inelastic e p scattering in perturbation theory, *Sov. J. Nucl. Phys.* **15**, 675 (1972).
- [40] G. Altarelli and G. Parisi, Asymptotic Freedom in Parton Language, *Nucl. Phys. B* **126**, 298 (1977).
- [41] I. I. Balitsky and L. N. Lipatov, The Pomeranchuk Singularity in Quantum Chromodynamics, *Sov. J. Nucl. Phys.* **28**, 822 (1978).
- [42] E. A. Kuraev, L. N. Lipatov, and V. S. Fadin, The Pomeranchuk Singularity in Nonabelian Gauge Theories, *Sov. Phys. JETP* **45**, 199 (1977).
- [43] L. V. Gribov, E. M. Levin, and M. G. Ryskin, Semihard Processes in QCD, *Phys. Rept.* **100**, 1 (1983).
- [44] A. H. Mueller and J.-w. Qiu, Gluon Recombination and Shadowing at Small Values of x, *Nucl. Phys. B* **268**, 427 (1986).
- [45] I. Balitsky, Operator expansion for high-energy scattering, *Nucl. Phys. B* **463**, 99 (1996), arXiv:hep-ph/9509348.
- [46] Y. V. Kovchegov, Small x F(2) structure function of a nucleus including multiple pomeron exchanges, *Phys. Rev. D* **60**, 034008 (1999), arXiv:hep-ph/9901281.
- [47] Y. V. Kovchegov, Unitarization of the BFKL pomeron on a nucleus, *Phys. Rev. D* **61**, 074018 (2000), arXiv:hep-ph/9905214.
- [48] R. Enberg, K. J. Golec-Biernat, and S. Munier, The High energy asymptotics of scattering processes in QCD, *Phys. Rev. D* **72**, 074021 (2005), arXiv:hep-ph/0505101.
- [49] S. Munier and R. B. Peschanski, Traveling wave fronts and the transition to saturation, *Phys. Rev. D* **69**, 034008 (2004), arXiv:hep-ph/0310357.

[50] S. Munier and R. B. Peschanski, Geometric scaling as traveling waves, *Phys. Rev. Lett.* **91**, 232001 (2003), arXiv:hep-ph/0309177.

[51] S. Munier and R. B. Peschanski, Universality and tree structure of high-energy QCD, *Phys. Rev. D* **70**, 077503 (2004), arXiv:hep-ph/0401215.

[52] E. Iancu, A. H. Mueller, and S. Munier, Universal behavior of QCD amplitudes at high energy from general tools of statistical physics, *Phys. Lett. B* **606**, 342 (2005), arXiv:hep-ph/0410018.

[53] R. Enberg, Saturation, traveling waves and fluctuations, *AIP Conf. Proc.* **792**, 307 (2005), arXiv:hep-ph/0507153.

[54] S. Munier, Statistical physics in QCD evolution towards high energies, *Sci. China Phys. Mech. Astron.* **58**, 81001 (2015), arXiv:1410.6478 [hep-ph].

[55] A. H. Mueller and S. Munier, Diffractive Electron-Nucleus Scattering and Ancestry in Branching Random Walks, *Phys. Rev. Lett.* **121**, 082001 (2018), arXiv:1805.09417 [hep-ph].

[56] Y. Yang, W. Kou, X. Wang, and X. Chen, Solitary wave solutions of FKPP equation using Homogeneous balance method(HB method), (2020), arXiv:2009.11378 [nlin.PS].

[57] X. Wang, Y. Yang, W. Kou, R. Wang, and X. Chen, Analytical solution of Balitsky-Kovchegov equation with homogeneous balance method, *Phys. Rev. D* **103**, 056008 (2021), arXiv:2009.13325 [hep-ph].

[58] X. Wang, W. Kou, G. Xie, Y.-P. Xie, and X. Chen, Exclusive vector meson production with the analytical solution of Balitsky-Kovchegov equation, *Chin. Phys. C* **46**, 093101 (2022), arXiv:2205.02396 [hep-ph].

[59] Y. Cai, X. Wang, and X. Chen, Analytic solution of the Balitsky-Kovchegov equation with a running coupling constant using the homogeneous balance method, *Phys. Rev. D* **108**, 116024 (2023), arXiv:2311.02672 [hep-ph].

[60] E. Iancu, K. Itakura, and L. McLerran, Geometric scaling above the saturation scale, *Nucl. Phys. A* **708**, 327 (2002), arXiv:hep-ph/0203137.

[61] F. D. Aaron *et al.* (H1, ZEUS), Combined Measurement and QCD Analysis of the Inclusive e+- p Scattering Cross Sections at HERA, *JHEP* **01**, 109, arXiv:0911.0884 [hep-ex].

[62] V. Andreev *et al.* (H1), Measurement of inclusive ep cross sections at high Q^2 at $\sqrt{s} = 225$ and 252 GeV and of the longitudinal proton structure function F_L at HERA, *Eur. Phys. J. C* **74**, 2814 (2014), arXiv:1312.4821 [hep-ex].

[63] K. Golec-Biernat, Saturation scale from the Balitsky-Kovchegov equation, in *12th International Workshop on Deep Inelastic Scattering (DIS 2004)* (2004) pp. 283–286, arXiv:hep-ph/0408255.

[64] E. Iancu and R. Venugopalan, The Color glass condensate and high-energy scattering in QCD, in *Quark-gluon plasma 4*, edited by R. C. Hwa and X.-N. Wang (2003) pp. 249–3363, arXiv:hep-ph/0303204.

[65] K. Kutak and A. M. Stasto, Unintegrated gluon distribution from modified BK equation, *Eur. Phys. J. C* **41**, 343 (2005), arXiv:hep-ph/0408117.

[66] D. Kharzeev and K. Tuchin, From color glass condensate to quark gluon plasma through the event horizon, *Nucl. Phys. A* **753**, 316 (2005), arXiv:hep-ph/0501234.

[67] P. Castorina, D. Kharzeev, and H. Satz, Thermal Hadronization and Hawking-Unruh Radiation in QCD, *Eur. Phys. J. C* **52**, 187 (2007), arXiv:0704.1426 [hep-ph].

[68] W. G. Unruh, Notes on black hole evaporation, *Phys. Rev. D* **14**, 870 (1976).

[69] S. K. Wong, Field and particle equations for the classical Yang-Mills field and particles with isotopic spin, *Nuovo Cim. A* **65**, 689 (1970).

[70] V. Mathieu, Gluon Mass, Glueballs and Gluonic Mesons, *PoS FACESQCD*, 002 (2010), arXiv:1102.3875 [hep-ph].

[71] V. Mathieu, Glueball spectroscopy, *Acta Phys. Polon. Supp.* **4**, 677 (2011).

[72] K. J. Golec-Biernat and M. Wusthoff, Saturation effects in deep inelastic scattering at low Q^{**2} and its implications on diffraction, *Phys. Rev. D* **59**, 014017 (1998), arXiv:hep-ph/9807513.

[73] D. E. Kharzeev and E. M. Levin, Deep inelastic scattering as a probe of entanglement, *Phys. Rev. D* **95**, 114008 (2017), arXiv:1702.03489 [hep-ph].

[74] M. Hentschinski and K. Kutak, Evidence for the maximally entangled low x proton in Deep Inelastic Scattering from H1 data, *Eur. Phys. J. C* **82**, 111 (2022), [Erratum: Eur.Phys.J.C 83, 1147 (2023)], arXiv:2110.06156 [hep-ph].

[75] M. Hentschinski, K. Kutak, and R. Straka, Maximally entangled proton and charged hadron multiplicity in Deep Inelastic Scattering, *Eur. Phys. J. C* **82**, 1147 (2022), arXiv:2207.09430 [hep-ph].

[76] M. Hentschinski, D. E. Kharzeev, K. Kutak, and Z. Tu, Probing the Onset of Maximal Entanglement inside the Proton in Diffractive Deep Inelastic Scattering, *Phys. Rev. Lett.* **131**, 241901 (2023), arXiv:2305.03069 [hep-ph].

[77] V. Andreev *et al.* (H1), Measurement of charged particle multiplicity distributions in DIS at HERA and its implication to entanglement entropy of partons, *Eur. Phys. J. C* **81**, 212 (2021), arXiv:2011.01812 [hep-ex].

[78] Z. Tu, D. E. Kharzeev, and T. Ullrich, Einstein-Podolsky-Rosen Paradox and Quantum Entanglement at Subnucleonic Scales, *Phys. Rev. Lett.* **124**, 062001 (2020), arXiv:1904.11974 [hep-ph].

[79] R. J. Glauber, Cross-sections in deuterium at high-energies, *Phys. Rev.* **100**, 242 (1955).

[80] V. N. Gribov, Interaction of Gamma Quanta and Electrons with Nuclei at High Energies, *Sov. Phys. JETP* **30**, 709 (1970).

[81] V. N. Gribov, Glauber Corrections and the Interaction between High-energy Hadrons and Nuclei, *Sov. Phys. JETP* **29**, 483 (1969).

[82] A. H. Mueller, Small x Behavior and Parton Saturation: A QCD Model, *Nucl. Phys. B* **335**, 115 (1990).

[83] A. H. Mueller, Parton saturation at small x and in large nuclei, *Nucl. Phys. B* **558**, 285 (1999), arXiv:hep-ph/9904404.

[84] Y. V. Kovchegov, Brief Review of Saturation Physics, *Acta Phys. Polon. B* **45**, 2241 (2014), arXiv:1410.7722 [hep-ph].

[85] N. Armesto, Nuclear structure functions at small x in multiple scattering approaches, in *38th Rencontres de Moriond on QCD and High-Energy Hadronic Interactions* (2003) arXiv:hep-ph/0305057.

[86] R. D. Woods and D. S. Saxon, Diffuse Surface Optical Model for Nucleon-Nuclei Scattering, *Phys. Rev.* **95**, 577 (1954).

- [87] Y. V. Kovchegov and E. Levin, *Quantum Chromodynamics at High Energy*, Vol. 33 (Oxford University Press, 2013).
- [88] J. L. Albacete and C. Marquet, Gluon saturation and initial conditions for relativistic heavy ion collisions, *Prog. Part. Nucl. Phys.* **76**, 1 (2014), arXiv:1401.4866 [hep-ph].
- [89] A. Accardi *et al.*, Electron Ion Collider: The Next QCD Frontier: Understanding the glue that binds us all, *Eur. Phys. J. A* **52**, 268 (2016), arXiv:1212.1701 [nucl-ex].
- [90] E. C. Aschenauer, S. Fazio, J. H. Lee, H. Mantysaari, B. S. Page, B. Schenke, T. Ullrich, R. Venugopalan, and P. Zurita, The electron-ion collider: assessing the energy dependence of key measurements, *Rept. Prog. Phys.* **82**, 024301 (2019), arXiv:1708.01527 [nucl-ex].
- [91] R. Abdul Khalek *et al.*, Science Requirements and Detector Concepts for the Electron-Ion Collider: EIC Yellow Report, *Nucl. Phys. A* **1026**, 122447 (2022), arXiv:2103.05419 [physics.ins-det].
- [92] A. Morreale and F. Salazar, Mining for Gluon Saturation at Colliders, *Universe* **7**, 312 (2021), arXiv:2108.08254 [hep-ph].